

## 바이오칩 제작 장치용 단결정 실리콘 마이크로 미러 어레이의 설계와 제작

장운호<sup>1</sup>, 이국녕<sup>2</sup>, 김용권<sup>1</sup>

<sup>1</sup>서울대학교 전기공학부, <sup>2</sup>서울대학교 응용화학부

### Design and fabrication of a single crystalline silicon micromirror array for biochip fabrication systems

Yun-Ho Jang<sup>1</sup>, Kook-Nyung Lee<sup>2</sup>, and Yong-Kweon Kim<sup>1</sup>

<sup>1</sup>School of Electrical Engineering and Computer Science, Seoul National University

<sup>2</sup>School of Chemical Engineering, Seoul National University

**Abstract** - Single crystalline silicon (SCS) was adopted for a reliable micromirror array of biochip fabrication applications. SCS has excellent mechanical properties and smooth surface, which is the best material for micromirror devices. The mirror array has  $16 \times 16$  micromirrors and each mirror has a  $120 \mu\text{m} \times 100 \mu\text{m}$  reflective surface. The micromirror has simple torsional beam springs and electrostatic force was used for driving. The designed tilting angle was  $9.6^\circ$ , and the tilting angles were measured according to applied voltages. The surface roughness was measured by a laser profiler. The response time was measured using He-Ne laser and position sensitive diode (PSD), and the lifetime was checked for reliability proof.

#### 1. Introduction

Micromirror arrays are currently applied to various optical systems such as projectors, spatial light modulators, and optical communication devices. Another application is a maskless photolithography for biochip fabrication [1]. They used a micromirror array for the generation of various light patterns, which are corresponding to each protein pattern. This scheme eliminated a lot of photomasks and improved flexibility of pattern generations. The application requires that the used micromirror have considerable reflective area than the commercially acquirable micromirror products ( $16 \times 16 \mu\text{m}^2$ ) to improve optical efficiency. Also a mirror's pitch should be controllable in the design stage to reduce the interference and increase the contrast between chemical reactive patterns.

The common requirements for the micromirror array are optically flat surface and stable structures. Traditionally, micromirror array has adopted aluminum as preferred material for its high reflective surface, easy fabrication and CMOS compatibility [2-4]. But a mirror plate fabricated with aluminum can be easily deformed when the mirror size is increased because of fabrication environments and residual stress of aluminum. Memory phenomena and mechanical fatigue are other obstacles to improve performances with aluminum micromirror array. In brief, aluminum is a good material for compatibility, but it is difficult to guarantee an optically flat surface and stable mechanical structures for the comparable large size micromirror.

To improve performances of micromirrors, some researches are focusing on single crystalline silicon (SCS) as optical and mechanical materials. SCS has optically flat surface, negligible residual stress and superior mechanical property [5-7]. So, SCS is the best material for the large micromirror fabrication. But it is difficult to fabricate complex micro-structures using SCS.

In this paper, to improve the optical and mechanical

performances of a micromirror array, SCS was adopted as a unique structural material for a mirror plate and torsional springs.

#### 2. Design

The schematic view of two micromirrors in an array is shown in Fig. 1. The mirror has two torsional springs and its structural material is all SCS. Aluminum is deposited on the SCS mirror plate for reflectivity improvements. The flat mirror plate could be attained by negligible residual stress of SCS and reliable torsional springs could be achieved by high yield strength of SCS.

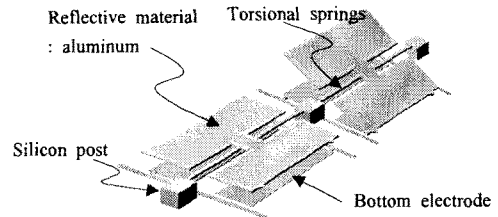


Figure 1.. Schematics of micromirrors : left mirror is in initial state, right one is in operation.

The torsional springs have loss of reflective area but simple structure leads to easy fabrication and analysis [8]. The silicon posts at the end of the springs are anodically bonded with a glass substrate. The posts support the mirror structure and conduct the electrical signal for operation.

The mirror plate and springs have the same thickness of about  $3 \mu\text{m}$ . A thin mirror plate is preferred because a small mass can increase resonance frequency and operational speed. But too thin plate is weak from the external force and it can be broken during fabrication processes. The length and width of the springs are  $70 \mu\text{m}$  and  $1 \mu\text{m}$ , respectively in the design step. The width and length of the mirror plate are  $120 \mu\text{m}$  and  $100 \mu\text{m}$ , respectively. The array is composed of  $16 \times 16$ , 256 micromirrors.

The right mirror in the figure 1 is addressed by electrostatic force between the mirror plate and the bottom electrode. The mirror plate is grounded and the bottom electrode is negative biased. The electrical potential of the mirror plate is supplied by springs, so all mirrors in the same row are equi-potential states. The bottom electrode is connected column by column. The mirror is inclined to the left or right at ten degrees and landing tips touch down the substrate when the pull-in voltage is applied.

The landing tips are designed to reduce contact area and in-use stick problems.

The pull-in voltage is affected by spring stiffness and the gap between mirror plate and bottom electrode. Because we have adopted conventional anodic bonding process, lapping and polishing process, silicon thickness can have some deviations. Among various parameters of a micromirror design, spring thickness and spring width are dominant factors for pull-in voltage calculations.

Figure 2 shows the pull-in voltage variations with respect to spring widths and thicknesses. Each line represents width and length combinations that yield the same pull-in voltages.

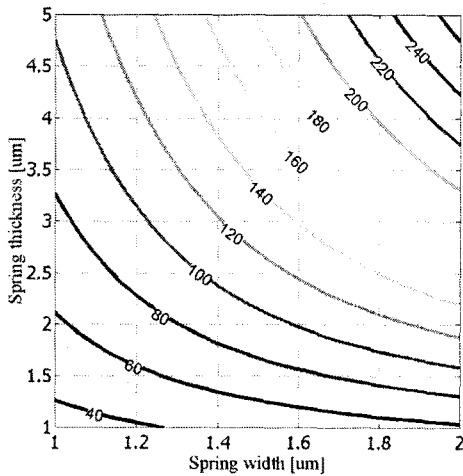


Figure 2. Pull-in voltage variations with respect to spring widths and thicknesses.

If the spring widths are varied from 1  $\mu\text{m}$  to 2  $\mu\text{m}$  and spring thicknesses are varied from 1  $\mu\text{m}$  to 5  $\mu\text{m}$ , the pull-in voltages exist between 40 V and 260 V.

### 3. Fabrication

Figure 3 shows the whole fabrication process.

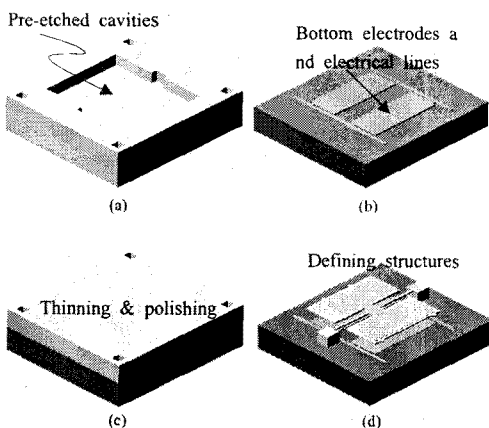


Figure 3. Fabrication process : (a) silicon deep etch for cavity formation, (b) electrode patterning on a glass wafer, (c) anodic bonding, thinning and polishing, (d) mirror structure patterning and release.

The first step is to form cavities (about 10  $\mu\text{m}$ ) on a silicon surface. The cavities are formed under a mirror plate and the springs for final release process. Evaporated aluminum (0.3  $\mu\text{m}$ ) is patterned as electrical lines and bottom electrodes on a glass wafer as shown in Fig. 3(b). Next, the silicon wafer is flipped over and bonded to a glass wafer in the alignment bonding system (EV501, EVG Co., Ltd.) as shown in Fig. 3(c). The desired thickness of silicon mirror plate is 3  $\mu\text{m}$ , therefore the silicon wafer thickness should be reduced up to 12  $\mu\text{m}$  after polishing step. We have lapped the silicon wafer chemically, and polished up to the desired thickness. Then, we deposit and pattern a thin aluminum layer to define the mirror structure including mirror plate, springs and post. Because one photolithography step defines the whole structures on the silicon wafer, there was no alignment errors between springs and mirror plates. After patterning the aluminum hard mask, the wafer is diced into several samples. Silicon structures are defined using silicon deep RIE. Because there is no sacrificial layer and the bottom cavities were pre-formed before the bonding process, all structures are released in the final etching step. Fluorocarbon (FC) film can be deposited to reduce sticking problems in-use stictions.

Figure 4 shows a microphotograph of fabricated micromirror array.

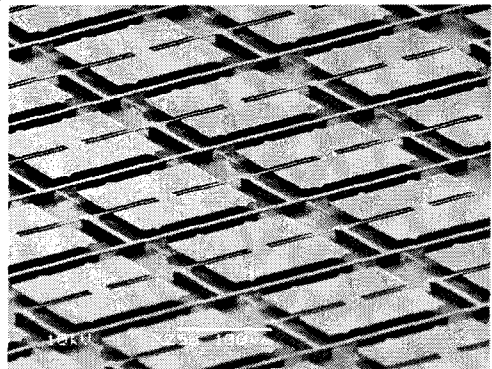
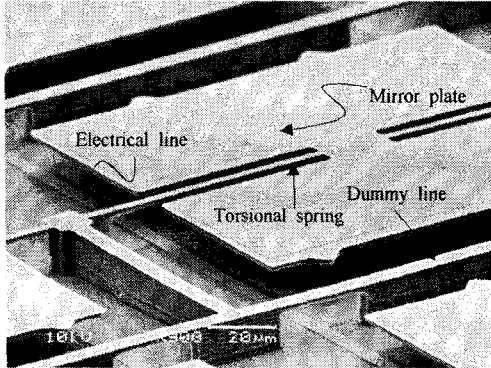


Figure 4. SEM photograph of fabricated SCS micromirror array.

The SCS micromirror array shows very uniform results and deformation is negligible. The fabricated silicon spring is thickened and widened than the designed values. The main factors for spring dimension variations are fabrication process errors. The spring pattern width on photolithography mask was slightly changed from the designed one, and aluminum hard mask pattern was changed from the designed patterns. Spring stiffness becomes 7 times large, which increase resonant frequency and pull-in voltage. Also the gap between mirror plate and bottom electrode has lower value than the designed one, because the gap is defined by deep silicon etcher. The deep etcher has fast etching capability of silicon ( $\sim 3 \mu\text{m}/\text{min}$ ), which makes it difficult to control desired depth. Since the electrical signals are delivered by springs to mirror plates, remaining mirrors could not operate if one mirror's springs are broken. We have added the dummy electrical lines parallel to springs for the spring damages.

Figure 5 shows an enlarged view of one mirror among the array. The mirror plate and torsional springs are patterned well, but some particles are observed on the surface. They may be happened during aluminum evaporation, which can be removed. The bottom electrodes and electrical lines are shown in figure 5. Electrodes and lines are not deformed during anodic bonding

process, because silicon cavities are defined around electrical lines during pre-etch step in figure 3 (a). The micromirror has 3.5 $\mu\text{m}$  thick mirror plate and springs. The width of springs was 1.56  $\mu\text{m}$ , which was significant reason for pull-in voltage increase up to 124 V, of which the design value was 73 V. High voltage could induce some side effects such as dielectric breakdown, therefore it should be reduced by controlling the spring widths.



**Figure 5.** Enlarged view of unit micromirror: SCS springs and mirror plate are patterned well. There are roughened surface on mirror plate, which would be aluminum particles during thermal evaporation. This can be removed by careful handling and additional cleaning steps.

The flat surface of the micromirror is also depicted in figure 6, which is measured using laser profiler (VF7500, Keyence Co., Ltd.). The averaged surface roughness ( $R_a$ ) measured by the laser profiler is less than 40 nm.

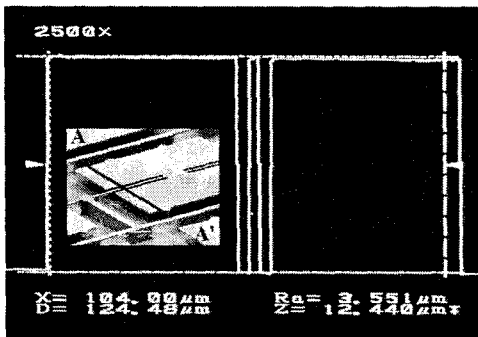


**Figure 6.** Laser profiler measurement: when scanned along AA', The height of the mirror surface from the bottom is measured 12.44 $\mu\text{m}$ .

#### 4. Results

Before characterizing properties of mirror array, we have to know mirror parameters such as pull-in voltages ( $V_p$ ), release voltage ( $V_r$ ), response time ( $t_p$ : pull-in time,  $t_r$ : release time) and life time for one micromirror. In this section, we are going to describe the theoretical expectations and the measurement results of an unit micromirror.

Pull-in voltage is determined by mechanical and electrical properties of the micromirror. The torsional spring stiffness and the geometry of electrodes affect the pull-in voltage. By combining the related equations, we can expect when a mirror touches down the substrate and restores to an original position. We have calculated the relationships between applied voltages and tilting angles, then compared the measurement data as

shown in figure 7.

Not considering the misalignment between the electrode and the mirror plate, pull-in voltage was calculated to 124 V. But 3  $\mu\text{m}$  misalignment was occurred during alignment bonding process, which decreases the pull-in voltage of 116 V as shown in figure 7. The tilting angle started to increase when the applied voltage increases and abruptly touched down a substrate when voltage reaches pull-in value. After the mirror was fully tilted, the gap between the electrode and the mirror plate so close that lower voltage than the pull-in voltage was sufficient for holding the mirror. The minimum voltage for release voltage is 40 V for both numerical analysis and experimental results. Since the mirror stays at the tilted state after the pull-in voltage is applied once, a holding voltage ( $V_h$ ) can be reduced lower than the pull-in voltage.

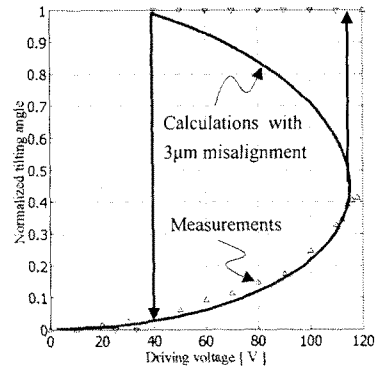


**Figure 7.** Normalized tilting angles according to driving voltages : The solid line represents numerical calculation with measured dimensions of springs and electrodes as shown in Table 1. Calculation also includes 3  $\mu\text{m}$  misalignment between the electrode and the mirror plate. Up triangles ( $\Delta$ ) mean tilting angles when the voltage increases, and down triangles ( $\nabla$ ) for decreasing voltages.

Next, we applied step input to bottom electrode while the mirror plate was grounded. The experiment was for measuring the response time and restoring time. The used experimental setup includes He-Ne laser and position sensitive diode (PSD) [9]. The laser beam is incident on the micromirror surface through the focusing lens. When the micromirror is driven by amplified voltage signals from a function generator and voltage amplifier, the reflected beam from the micromirror surface reaches the PSD detectors. The PSD translate the position data into voltage signals, which is plotted with a digital oscilloscope.

Figure 8 shows the oscilloscope outputs when the driving voltage is turned on and off. In figure 8 (a), the mirror is switched on and the fully tilted. The response time for pull-in state is about 25  $\mu\text{sec}$  and there are no rebounding phenomena. When the voltage is turned off, the mirror is released and back to an initial state. There are oscillations during settling, and the settling time is about 500  $\mu\text{sec}$ . Since the mirror is oscillated with own resonant frequency, the resonant frequency can be assumed as 32 kHz, which is agreed well with ANSYS simulations. The long settling time could be an obstacle for fast operations. Also the micromirrors in long oscillations would reflect the incident light to the patterns after the driving signal is turned off, which could reflect the undesired light and limit the contrast between biochip patterns. To remove oscillations, the opposite side electrode will be biased at the moment the driving electrode is turned off.

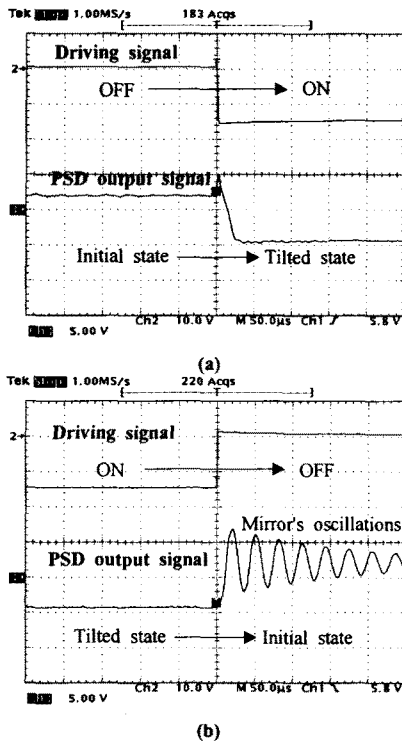


**Figure 8.** Step response measurements: (a) When the voltage is applied abruptly, the mirror is tilted and the tips touches down the substrate. (b) When the voltage is removed, the mirror is released from the electrostatic force

We have experimented life time using same experimental setup shown in figure 8. As the mirror was driven by square function, the output position signal was observed by the oscilloscope. The position signal was not changed after  $3.5 \times 10^8$  cycles.

### 5. Conclusion

Micromirrors that have SCS mirror plate and SCS torsional springs are designed and fabricated using silicon deep etch and anodic bonding process. The silicon membrane is thinned for the mirror plate and the springs. The average surface roughness is below 40 nm. The pull-in voltage was 116 V and minimum holding voltage after pull-in was about 40 V. The pull-in time and release time were 25  $\mu$ sec and 500  $\mu$ sec, respectively. Even though the mirror operated  $3.5 \times 10^8$  cycles, there was no degradation. The fabricated SCS micromirror array has potential applications as stable light modulators in micro optical systems including biochip fabrication systems.

### Acknowledgement

This work was supported by the Korea Research Foundation Grant (KRF-2002-041-D00228).

### [References]

[1] K. N. Lee, D. S. Shin, Y. S. Lee and Y. K. Kim, "Micromirror array for protein micro array fabrication", *J. Micromech. Microeng.* vol. 13, pp. 474-481, 2003.  
 [2] L. J. Hornbeck, "Deformable micro spatial light modulators, Spatial light modulators and applications III", *SPIE Critical Reviews* vol. 1150, pp. 86-102, 1989.  
 [3] P. F. Kessel, L. J. Hornbeck, R. E. Meier and M. R.

Douglass, "A MEMS-Based Projection Display", *Proc. of the IEEE*, vol. 86, pp. 1687-1704, 1998.

[4] Y. H. Jang and Y. K. Kim, "Design and fabrication and characterization of an electromagnetically actuated addressable out-of-plane micromirror array for vertical optical source applications", *J. Micromech. Microeng.* vol. 13, pp. 853-863, 2003.  
 [5] S. Haasl, F. Niklaus and G. Stemme, "Arrays of monocrystalline silicon micromirrors fabricated using CMOS compatible transfer bonding", in *Proc. 16th Annu. International Conference on MEMS*, Kyoto, Japan, pp. 271-274, 2003.  
 [6] M. Dokmeci, S. Bakshi, M. Waelti, A. Pareek, C. Fung and C. Mastrangelo, "Bulk micromachined electrostatic beam steering micromirror array", in *Proc. International Conference on Optical MEMS*, Lugano, Switzerland, pp. 15-16, 2002.  
 [7] V. P. Jaecklin, C. Linder, J. Brugger, N. F. de Rooji, J. M. Moret and R. Vuilleumier, "Mechanical and optical properties of surface micromachined torsional mirrors in silicon, polysilicon and aluminum", *Sensors and Actuators, Phys. A* vol. 43 pp. 269-275, 1994.  
 [8] J. W. Judy and R. S. Miller, "Magnetically actuated, addressable microstructures," *J. Microelectromechanical Systems*, vol. 6, no. 3, pp. 249-256, 1997.  
 [9] S. W. Chung and Y. K. Kim, "Measurement of a fabricated micro mirror using a lateral effect position sensitive photodiode", *IEEE Trans. Industrial electronics*, vol. 45, no. 6, pp. 861-865, 1998.